Local collective memory from ratiometric signaling outperforms cellular gradient sensing limits

Debraj Ghose *[1], James Nolen *[2], Kaiyun Guan[3], Timothy C. Elston[4], and Daniel J. Lew †[5]

[1]Wyss Institute for Biologically Inspired Engineering, Harvard University, Boston, MA, 02215, USA
[2]Department of Mathematics, Duke University, Durham, NC, 27708, USA
[3]Curriculum in Bioinformatics and Computational Biology, University of North Carolina at Chapel Hill, Chapel Hill, NC, 27599, USA
[4]Department of Pharmacology and Computational Medicine Program, University of North Carolina at Chapel Hill, Chapel Hill, NC, 27599, USA
[5]Department of Biology, Massachusetts Institute of Technology, Cambridge, MA, 02139, USA

March 2025

Abstract

Cells excel at interpreting noisy chemical gradients during fertilization, development, and immune responses, but the mechanisms underlying this remarkable ability remain poorly understood. Classical models for gradient sensing assume that information is derived solely from ligand-bound receptors, but cells can also utilize information from unbound receptors. Here, we first derive the physical limit for instantaneous gradient detection by a distribution of receptors on a sphere. Surprisingly, we find that a ratiometric biochemical strategy, which compares spatial distributions of active (bound) and inactive (unbound) receptors, can surpass this physical limit. Using theory and simulations, we show this enhancement stems from a local collective memory encoded by downstream proteins that average receptor states sampled over time. Such memory-driven averaging allows cells to reliably interpret gradient direction despite receptor scarcity or noisy conditions, demonstrating how ratiometric sensing mechanisms could broadly enhance cellular responses to directional cues from the environment.

Significance Statement

Cells detect chemical gradients using receptors on their surface to guide essential processes like fertilization, immune responses, and organismal development. However, chemical environments are often noisy and complex, and it remains unclear how cells can accurately interpret these signals. We show that by using information from inactive as well as active receptors, a cell can average each receptor's state over time and store that information in a population of downstream signaling proteins near the receptor. This strategy improves gradient sensing accuracy even when receptors are scarce or gradients are noisy, offering a path to improved engineering of microscale biosensors or drug-delivery devices that can orient in complex chemical landscapes.

Introduction

Cells are exceptional at extracting directional information from their chemical environment, often under complex and noisy conditions that demand high accuracy. Some of the earliest direct experimental evidence that cells respond to chemical gradients emerged in the late 19th century, with studies involving bacteria clustering near oxygen-rich zones [1, 2] and plant spermatozoids finding female reproductive organs [3]. Since then, chemotactic or chemotropic responses by cells or subcellular components have been documented in pollen tube guidance [4, 5], protozoa [6–8], fungi [9–14], immune cells [15, 16], animal sperm [17–19], neurons [20, 21], developmental processes [22], cancer cells [23–25], and many other systems. Together, these observations broadly illustrate the diverse scenarios under which gradient-driven cell guidance occurs.

In all cases, cells detect chemical signals through binding to cell-surface receptors that engage internal signaling pathways [26, 27]. Using these receptors, a cell can in principle estimate the direction of a ligand gradient by measuring the difference in chemical concentration across its width. However, the rapid movement of fast-swimming cells like bacteria or sperm causes them to collide with ligand molecules more often at their front than at their back. This differential collision rate can make the concentration gradients they perceive across their width appear hundreds of times steeper than the actual environmental gradients [28]. Such cells have developed "temporal sensing" strategies that monitor concentration changes over time as they move through space. In contrast, a large majority of larger eukaryotic cells, which are slower moving or non-motile, employ a "spatial sensing" strategy that compares concentrations of chemicals on different sides of the cell to infer gradient direction. Once a direction is established, eukaryotic cells can polarize and move or grow toward (or

*These authors contributed equally to this work.
†Corresponding author: djlew@mit.edu

away from) higher ligand concentrations. Even so, these spatial measurements can be thwarted by noise, low signal from shallow gradients, or complex gradient landscapes, especially for smaller cells. A well-appreciated strategy to enhance low signals over noise in the case of scalar measurements is to use time-averaging of receptor signals. However, molecular mechanisms for averaging directional information about ligand gradients remain poorly understood.

Previous theoretical efforts have studied fundamental physical limits to both absolute ligand concentration measurement [28–30] and gradient measurement [31, 32], grounded in considerations of ligand-binding noise. Many of these analyses assume that only ligand-bound receptors provide relevant information. Yet in real cells, receptors exist in both inactive (unbound) and active (ligand-bound) states, and it may be advantageous to incorporate information from both. Inspired by the mating response of budding yeast, we consider a *ratiometric* ligand-sensing strategy in which downstream signaling depends on the ratio of active to inactive receptor levels [33, 34]. Such a system enables a cell to interpret its environment by extracting signals from both bound and unbound receptor states.

In this study, we derive the physical limits on the accuracy of gradient detection for a three-dimensional sphere populated with randomly distributed receptors, and compare classical and ratiometric signaling mechanisms. We show that the ratiometric approach outperforms classical models and can even surpass theoretical bounds for instantaneous receptor measurements, owing to a local collective memory of past receptor states encoded by downstream signaling proteins. Our results show how cells could exploit ratiometric mechanisms to outperform classical gradient-sensing limits, and suggest strategies for designing synthetic gradient sensing systems.

Results

Using spatial information from inactive as well as active receptors enables more accurate inference of gradient direction

To evaluate the potential benefits or pitfalls of a ratiometric sensing strategy, we need a metric that tells us how accurately a theoretical cell can infer the direction of a ligand gradient. Previous studies have compared the ligand concentrations sensed by the front and back halves of a cell, thereby determining whether the difference (signal) exceeds the noise [28, 31]. However, splitting the cell in half presupposes prior knowledge of the axis along which concentration changes occur. Because a real cell generally does not have that information, other work has instead estimated the cell's "best guess" of the gradient direction by summing the vectors from the cell center to all active receptors [32, 35] (Fig. 1A).

The resulting active receptor vector, V_{RL}, provides an estimate of the gradient direction pointing towards the highest ligand concentration. Comparing V_{RL} with the actual gradient direction provides an angular measure of how closely the cell's guess matches reality. In principle, one could also compute the gradient direction from inactive receptors alone to produce a "best guess" vector V_R pointing towards the lowest ligand concentration. To combine information from both active and inactive receptors, we can calculate $V_C = V_{RL} - V_R$ (Fig. 1A).

In what follows, we simulate a spherical cell in three dimensions, with N_R receptors randomly distributed over its surface. As receptor diffusion on the membrane is slow, especially in budding yeast ($\sim 0.0005\mu m^2/s$) [33, 36], we neglect it. Receptors can switch between active and inactive states at rates that depend on local ligand concentration $C(x)$; in statistical equilibrium, the probability of a receptor being active at a given time is

$$\mathbb{P}\big(\text{receptor at } x \text{ is active}\big) \;=\; \frac{C(x)}{C(x)+K_d}. \tag{1}$$

We expose the spherical cell to linear ligand gradients of the form

$$C(x,\theta) \;=\; C_0(1+b(x\cdot\theta)/L), \tag{2}$$

where θ is the direction vector, C_0 is the mid-point (average) ligand concentration, and x is a point on the sphere of radius L centered at the origin. We first assume the gradient is centered around K_d (i.e. $C_0 = K_d$). Molecular noise from ligand binding/unbinding causes estimates of the gradient direction θ to fluctuate over time. We quantify directional accuracy by examining the empirical cumulative distribution functions for the angular deviation of $\bar{V}_{RL}$, $-\bar{V}_R$, and $\bar{V}_C$ (the normalized summed vectors) relative to θ across many independent realizations (Fig. 1 B i-iii).

As $\bar{V}_c$, $\bar{V}_{RL}$, and $-\bar{V}_R$ are each statistical estimators of gradient direction, we can compare them to the Cramér-Rao bound [37], which provides a rigorous lower bound on the variance of $\bar{V}$ from the true direction θ, relative to the signal strength $\|\mathbb{E}[\bar{V}]\|$. This bound on the "noise-to-signal ratio" (NSR) takes the form

$$NSR \geq \text{trace}\big(\mathcal{I}^{-1}\big) \tag{3}$$

where $\mathcal{I}$ is a Fisher information matrix that can be computed numerically. In the weak-signal regime (small slope, b) this bound is approximated by

$$NSR \geq \text{trace}\big(\mathcal{I}^{-1}\big) \;\approx\; \frac{6}{N_R\, b^2}\,\frac{\big(C_0+K_d\big)^2}{K_d\, C_0}, \tag{4}$$

which shows that the minimal achievable variance in the estimated direction decreases proportionally to $1/N_R$ and depends inversely on b^2, thereby highlighting the advantage of stronger gradients and higher receptor number (details of this bound and a derivation of (4) appear in the Supplementary Information). A related bound is derived in [32] for a different model.

A comparison with this theoretical lower bound (Equation 3) shows that the estimates $\bar{V}_c$, $\bar{V}_{RL}$, and $-\bar{V}_R$ are indeed noisy, leaving ample room for improvement, especially at low N_R (Fig. 1 C). At high N_R, the variance of $\bar{V}_c$, $-\bar{V}_R$, and $\bar{V}_{RL}$ decrease along with the Cramér-Rao bound, which scales as $1/N_R$ (Fig. 1C). The variance of the combined estimate $\bar{V}_C$ is roughly half that of either $\bar{V}_{RL}$ or $\bar{V}_R$, as expected from the $1/N_R$ scaling of the optimal variance and the fact that roughly half of the receptors are active in this regime. Effectively, $\bar{V}_C$ draws on twice the data that either $\bar{V}_{RL}$ or $-\bar{V}_R$ alone can provide, demonstrating that incorporating both ligand-bound and unbound receptors significantly enhances directional sensing.

Using spatial information from inactive receptors broadens the range of ligand gradients that can be reliably decoded

To determine whether these conclusions extend to other gradients, we simulated a range of linear gradients covering different mean ligand concentrations (Fig. 1D). As the ligand concentration rises, saturation becomes more pronounced, so a larger fraction of receptors are active and the signal is diminished. Consistent with that expectation, V_{RL} performs increasingly poorly at higher concentrations (Figure 1D i-iii). Though $-V_R$ also degrades at high concentrations, it does so differently from V_{RL}. When the gradient is centered below K_d, V_{RL} outperforms $-V_R$ (Fig. 1D i); at K_d, V_{RL} and $-V_R$ perform similarly (Fig. 1D iii); above K_d, $-V_R$ becomes superior (Fig. 1D iii). This pattern suggests that at low ligand concentrations, the scarce active receptors provide more information than the many inactive ones, whereas at high ligand concentrations, the fewer inactive receptors carry more information. The combined vector V_C performs as well as or better than either V_{RL} or $-V_R$ across the same tested range (Fig. 1 D i-iii). Hence, pooling signals from both active and inactive receptors broadens the range of gradients that can be decoded accurately.

Ratiometric sensing biochemistry can improve inference of ligand gradient direction to an unexpected degree

Until now, we have imagined that a cell could apply some procedure to calculate V_C (and extract the direction $\bar{V}_C$), but we neglected the actual biochemical processes by which such calculations necessarily arise. Indeed, any downstream signaling step cannot preserve 100% of the information available at an earlier step, as noise in the interpretation mechanism will inevitably degrade the signal. For the ubiquitous and large family of G protein coupled receptors (GPCRs) that signal to downstream heterotrimeric G proteins, the biochemical mechanisms have been elucidated, and we consider here a simplified scheme in which a cell contains N_G G proteins that diffuse on the 2D surface of the spherical cell and can become activated or inactivated. Activation occurs with some probability upon collision between a diffusing inactive G protein and a ligand-bound receptor.

Following [33], we explore two different models of G protein inactivation (Fig. 2). In the *classical* model, inactivation occurs at a spatially uniform rate that is independent of receptor occupancy (Fig. 2A). In contrast, in the *ratiometric* model, inactivation occurs with some probability upon collision between a diffusing active G protein and an unbound receptor (Fig. 2B). We adjust the uniform inactivation rate of the classical model so that matched classical and ratiometric simulations have the same steady-state abundance of active G proteins, thereby permitting fair comparisons [33]. Note that unlike the ratiometric model, the classical model does not incorporate information about the spatial distribution of inactive receptors.

In a ratiometric system, because ligand binding simultaneously increases the number of active receptors and decreases the number of inactive receptors, these opposing effects can amplify fluctuations due to molecular noise [38]. Indeed, [39] suggests that for a fixed ligand concentration, a cell's measurement of ligand levels is noisier under a ratiometric (or "concerted") mechanism than under the classical mechanism.

Nevertheless, this need not imply that direction sensing becomes less reliable. For example, suppose (F_r, B_r) and (F_c, B_c) are pairs of random variables representing the active G protein concentration near the cell's front (F) and back (B), under the ratiometric (r) or classical (c) mechanisms. It may be that $CV(F_c) < CV(F_r)$ and $CV(B_c) < CV(B_r)$, yet $F_r - B_r > F_c - B_c$ (or $F_r/B_r > F_c/B_c$) still holds with high probability. (CV denotes coefficient of variation.) In other words, although the "signal" at any given location may be noisier in the ratiometric mechanism, the overall direction information (e.g., the difference $F - B$ or ratio F/B) can remain more robust compared to the classical system (see Section 5 and Fig. S6–S8 in the Supplement).

To compare sensing between classical and ratiometric systems, we calculated resultant vectors for active G proteins in a manner analogous to the previously discussed active receptor vector V_{RL} (Fig. 1A). We denote the resultant vectors of active G proteins under the ratiometric and classical models by V_G^r and V_G^c, respectively, and their normalized directions by $\bar{V}_G^r$ and $\bar{V}_G^c$. For ligand gradients near the receptor K_d, the ratiometric model (V_G^r) yields a significantly more accurate estimate of the gradient direction than the classical model (V_G^c) as demonstrated by temporal traces (Fig. 2C) (Movies S1-S6) and cumulative distribution functions (Fig. 2D) of V_G^c direction relative to gradient direction. Consequently, ratiometric sensing markedly enhances the accuracy of spatial gradient detection, even though it may sacrifice some accuracy in estimating the overall ligand concentration.

We next compared the performance of V_G^r to that of the combined receptor vector V_C. In simulations with many

receptors (large N_R), the receptor-based vector V_C performed better than V_G^r (Fig.3A). This was expected, as the smaller number of G proteins ($N_G = 2500$) cannot retain all directional information from the larger number of receptors ($N_R = 6000$). However, as N_R decreased, V_C became increasingly susceptible to stochastic noise. Remarkably, V_G^r retained its performance at lower N_R values (Fig.3A, B), so that below some threshold in receptor count (approx. $N_R < 1280$), V_G^r actually outperformed V_C (Fig. 3C). Even more unexpectedly, for sufficiently low N_R (approx.$N_R < 800$), V_G^r performed better than the theoretical Cramér–Rao bound derived for the variance of V_C (Fig.3C). While these simulations were carried out using custom code written in MATLAB 2024a, the surprising results were verified independently using the particle-based simulator SMOLDYN (Figures S1 and S2). Thus, ratiometric G protein signaling can continue to provide accurate directional information despite receptor scarcity.

G proteins enhance gradient sensing by collectively sampling past receptor states

How can the G protein vector V_G^r outperform the combined receptor vector V_C? This observation suggests that the instantaneous distribution of active G proteins can carry more information than that of the receptors alone. Because receptors and G proteins occupy binary states, the G protein population can only carry additional information if $N_G > N_R$. Indeed, reducing the number of G proteins lowers the accuracy of V_G^r (Fig. 4A).

We propose that when $N_G > N_R$, G proteins capture additional information by repeatedly sampling receptor states. The cartoon in Figure 4C illustrates how this sampling could average fluctuations for a single receptor that stochastically switches between active and inactive states with characteristic time scale λ^{-1}, where

$$\lambda \;=\; k_{\text{on}}\, C \;+\; k_{\text{off}}, \tag{5}$$

k_{on} and k_{off} are on/off rates of ligand binding, and C is the local ligand concentration. As the receptor is switching states, n G proteins encounter the receptor at randomly distributed intervals with mean collision time τ. While the mean fraction of active G proteins (A_n) would be the same as the fraction of time the receptor is on (p_R), the variance of A_n would increase with decreasing λ. This is because lower λ would lead to the receptor spending more time in a given state, causing states of G proteins that recently encountered the receptor to become more correlated. In our simulated scenario, the mean collision time is

$$\tau \;\propto\; \frac{L^2}{N_R\, D_G}\, \ln\!\left(\frac{\delta}{r_*}\right), \tag{6}$$

where L is the cell's linear dimension (e.g. radius), D_G is the G protein diffusion constant, N_R is number of receptors, r_* is the receptor interaction radius, and δ is the typical receptor spacing.

Using definitions of λ and τ in equations 5 and 6, we derive an expression for variance of A_n (see Supplement):

$$\text{Var}(A_n) \;=\; p_R(1-p_R)\left[\tfrac{1}{n} \;+\; \left(1-\tfrac{1}{n}\right)\tfrac{1}{1+\lambda\,\tau}\right]. \tag{7}$$

Thus, faster receptor switching (larger λ) or slower G protein diffusion (larger τ) raises $\lambda\tau$, which lowers $\text{Var}(A_n)$ and improves the accuracy of estimating p_R (Fig. 4D). Overall, because G proteins in the ratiometric mechanism store past receptor states between collisions, they collectively surpass what can be inferred from any single snapshot of the receptor distribution (Fig. 4E). In Section 4 of the Supplement we explain how this mechanism works when there are multiple receptors distributed across the cell surface, and we show how the time scales λ^{-1} and τ affect the reliability of the direction estimate V_G^r.

This analysis also supports the striking observation that the noise-to-signal ratio of V_G^r is relatively insensitive to N_R across a range of values of N_R that extends well below N_G. Figure 2E, Figure 3C, and Figure 3A each demonstrate this insensitivity over a broad range. In Figure 3C, at low receptor number, V_G^r maintains a low noise-to-signal ratio—even below what is theoretically achievable for V_C at the same N_R (i.e., below the Cramér–Rao bound for V_C). This occurs because historical sampling of receptor states enables V_G^r to effectively sample more receptors, thus encoding more information than is available in the instantaneous receptor states. In Figure 4A, as N_G increases (with N_R fixed), the estimate V_G^r becomes more accurate than V_C, the noise-to-signal ratio of V_G^r ultimately dropping below the Cramér–Rao bound for V_C.

In summary, the collective "memory" afforded by the G proteins' repeated sampling of receptors enables them to locally average past receptor states, which substantially enhances gradient sensing. This effect is most pronounced when the number of G proteins significantly exceeds the number of receptors, because each receptor can be sampled by multiple G proteins. By incorporating both bound and unbound receptor information over time, ratiometric signaling achieves greater directional accuracy than classical models relying solely on active receptors. Such benefits are particularly relevant when gradients are shallow or receptors are sparse, where noise could otherwise overwhelm directional cues.

Responsiveness to changing gradients

In the preceding discussion, we assumed that ligand gradients were stable over time. However, this is not always the case, and many cells must adapt to changing gradients such as when neutrophils chase bacteria, social amoebae collectively generate fruiting bodies, or budding yeast track their mating partners [10, 40, 41]. To assess how different parameters affect a cell's ability to adapt to changing gradients, we performed simulations in which we allowed V_G^r to reach steady state in a gradient, and then reversed the gradient direction by 180 degrees. We then

measured the time required for V_G^r to equilibrate to the new gradient direction. We found that increasing receptor switching rates not only enhances steady-state gradient sensing performance (Fig. 4E) but also improves the cell's ability to adapt quickly to new gradient directions (Fig. 4F). In contrast, increasing the G protein diffusion constant reduces steady-state accuracy (Fig. 4F) but accelerates adaptation to changing gradients (Fig. 4F). This occurs because faster diffusion allows G proteins to update their states more rapidly. Likewise, allowing G proteins to update their states more often by increasing receptor density N_R also accelerates adaptation (Fig. 4F). Thus, cells can modulate receptor kinetics and diffusion rates to balance precise steady-state sensing against rapid adaptation: faster receptor kinetics simultaneously boosts steady-state performance and adaptation speed, whereas higher diffusion constants reduce spatial accuracy yet facilitate quicker updates.

Discussion

Ratiometric signaling in the budding yeast system

Gradient decoding is most challenging when cells are small, gradients are shallow, and chemical concentrations are low, but yeast cells find mates despite encountering all of these challenges. An effective strategy to extract signals from noisy measurements would be to integrate concentration measurements over time, allowing time averaging to reduce the noise (fluctuations) without affecting the signal (gradient). However, once a chemical has bound to a cell-surface receptor, diffusion of the receptor-ligand complex would degrade the information about the location where the binding took place. Such blurring can limit the interval over which time-averaging is effective for directional sensing [35]. This is particularly problematic for systems like yeast pheromone sensing, where ligand-receptor complexes can persist for several minutes. Interestingly, yeast cells severely limit receptor diffusion ($D < 0.0005\ \mu m^2/s$), perhaps mitigating this problem [33]. However, with very slow receptor diffusion, receptors often accumulate non-uniformly on one side of the cell [33, 42–44]. Non-uniform receptor distributions in turn can lead to spatial patterns of ligand-receptor complexes that do not accurately reflect the spatial distribution of ligands in the environment.

Yeast cells appear to use a ratiometric sensing strategy to compensate for non-uniform receptor distributions [33]. Ligand binding to receptors promotes activation of G proteins that are then turned off by RGS proteins (Sst2 in yeast). In classical signaling models, G protein inactivation occurs in a receptor-independent manner, but in yeast cells the RGS protein is bound to inactive receptors [42]. Thus, whereas active receptors promote signaling, inactive receptors inhibit signaling, and the net signal reflects the ratio of active to inactive receptors [34]. If receptors are concentrated in some region of the cell surface, both active and inactive receptors may be locally enriched, so ratiometric sensing can allow the cell to accurately infer the local ligand distribution by compensating for the local receptor abundance. Interestingly, we find that, in addition to extracting information from both active and inactive receptors, ratiometric sensing could also enable a cell to interpret temporally averaged receptor states over time.

Noise in concentration measurement from ratiometric signaling

In principle, ratiometric signaling could be a widely applicable strategy to improve the detection of spatial gradients, especially when gradient concentrations are near the ligand-receptor K_d. It seems intuitively plausible that a cell capable of using information about the spatial distributions of inactive as well as active receptors would have a firmer basis to infer the spatial distribution of ligand than a cell whose only information comes from the active receptors. However, as discussed in the Supplement and shown in [38,39], ratiometric signaling can be less accurate at sensing absolute concentration. Nevertheless, we find that despite being worse at sensing ligand concentration, the ratiometric strategy provides more accurate gradient sensing by enabling acquisition of information from both active and inactive receptors as well as locally averaging receptor signals over time.

We show that ratiometric signaling outperforms classical signaling, even at very low receptor numbers when less than 0.02% of the cell surface is covered in receptors. Notably, these conditions resemble scenarios where cells initially populate their membranes with specific receptors—such as in lymphocytes like B cells, which upregulate receptors upon transitioning between germinal center zones; and in various developmental contexts where cells switch states and begin expressing new receptors [45, 46]. In such scenarios, ratiometric signaling could enable reliable gradient detection with lower receptor density, all while resisting misdirection by local fluctuations in receptor localization or ligand availability.

Mechanism underlying gradient detection accuracy by ratiometric signaling

One of our most intriguing observations was that ratiometric signaling could outperform the theoretical bound for gradient direction estimates that use only receptor snapshots at a single moment in time. This surprising advantage arises because downstream molecules—specifically, diffusing G proteins—act as a form of collective molecular memory. As each G protein updates its activity state only upon encountering a receptor, it encodes receptor information from an earlier time point. A population of G proteins that do this for both active and inactive receptors can smooth out short-lived fluctuations and enhance the fidelity of direction estimates. In effect, G proteins collectively time-average receptor states, allowing the cell

to extract more robust spatial information than would be possible from instantaneous receptor states alone.

In ratiometric signaling, two parameters critically balance directional accuracy and adaptive speed: the switching rate (λ) of receptor-ligand binding and the diffusion coefficient (D_G) of G proteins. Increasing λ enhances collective local averaging by G proteins (Fig. 4E), improving steady-state gradient detection, and promotes faster adaptation to shifting gradients (Fig. 4F). In contrast, raising D_G weakens local averaging and diminishes steady state-gradient detection (Fig. 4E). But higher D_G accelerates adaptation to changing signals, as more frequent receptor–G protein collisions swiftly update G protein states in response to new external conditions (Fig. 4F). Together, these trade-offs highlight how ratiometric signaling can be tuned to optimize either accuracy or speed, as required by the biological context.

Broader relevance of ratiometric signaling in responding to directional cues

It is not known whether receptors other than GPCRs can engage ratiometric signaling pathways. However, the principle underlying the averaging of upstream signals by more abundant downstream components may extend beyond receptor signaling, particularly in systems where both active and inactive states of upstream proteins convey meaningful information. In MAPK cascades, downstream kinases often exceed the abundance of their upstream regulators, exemplified by Raf in mammalian ERK pathways [47], B-Raf in cancer signaling contexts [48], and Ste11 in yeast mating responses [49]. These systems possess features that suggest the potential for ratiometric measurement-driven averaging to enhance accuracy and robustness.

Overall, our work suggests that ratiometric signaling mechanisms provide a powerful framework for cells to interpret directional receptor information and mitigate noise. The ability to sample both active and inactive states, combined with downstream emergent molecular memory, enables more accurate direction finding than that achieved by classical signaling mechanisms. These results offer testable predictions for experimental systems and may help clarify why some cells have a higher abundance of downstream proteins in signaling cascades.

Acknowledgments

This work was supported by NIH/NIGMS grant R35GM122488 to D.J.L. D.G. was supported by the Alfred P. Sloan Foundation's Matter-to-Life program.

References

[1] Th W Engelmann. Neue methode zur untersuchung der sauerstoffausscheidung pflanzlicher und thierischer organismen. *Archiv für die gesamte Physiologie des Menschen und der Tiere*, 25(1):285–292, 1881.

[2] Gerhart Drews. Contributions of Theodor Wilhelm Engelmann on phototaxis, chemotaxis, and photosynthesis. *Photosynthesis Research*, 83(1):25–34, January 2005.

[3] Wilhelm Pfeffer. *Locomotorische Richtungsbewegungen durch chemische Reize:(Aus den" Untersuchungen aus dem botanischen Institut zu Tübingen Bd. I. Heft 3 p. 363-482).* W. Engelmann, 1884.

[4] Hans Molisch. Zur physiologie des pollens, mit besonderer rücksicht auf die chemotropischen bewegungen der pollenschläuche. *Sitzungsberichte*, 102:423–448, 1893.

[5] Bengt Lidforss. Untersuchungen über die reizbewegungen der pollenschläuche. 1. der chemotropismus. *Zeitschrift für Botanik*, 1(7):443–496, 1909.

[6] Herbert Spencer Jennings. *Contributions to the study of the behavior of lower organisms.* Number 16. Carnegie institution of Washington, 1904.

[7] John Tyler Bonner and LJ Savage. Evidence for the formation of cell aggregates by chemotaxis in the development of the slime mold dictyostelium discoideum. *Journal of Experimental Zoology*, 106(1):1–26, 1947.

[8] Theo M Konijn, JG Van De Meene, John T Bonner, and David S Barkley. The acrasin activity of adenosine-3', 5'-cyclic phosphate. *Proceedings of the National Academy of Sciences*, 58(3):1152–1154, 1967.

[9] J E Segall. Polarization of yeast cells in spatial gradients of alpha mating factor. *Proceedings of the National Academy of Sciences*, 90(18):8332–8336, September 1993. Publisher: Proceedings of the National Academy of Sciences.

[10] Debraj Ghose, Katherine Jacobs, Samuel Ramirez, Timothy Elston, and Daniel Lew. Chemotactic movement of a polarity site enables yeast cells to find their mates. *Proceedings of the National Academy of Sciences*, 118(22), June 2021. Publisher: National Academy of Sciences Section: Biological Sciences.

[11] Jayme M. Dyer, Natasha S. Savage, Meng Jin, Trevin R. Zyla, Timothy C. Elston, and Daniel J. Lew. Tracking shallow chemical gradients by actin-driven wandering of the polarization site. *Current Biology*, 23(1):32–41, 2013.

[12] Karen M Snetselaar, Michael Bölker, and Regine Kahmann. Ustilago maydismating hyphae orient their growth toward pheromone sources. *Fungal genetics and biology*, 20(4):299–312, 1996.

[13] Arthur Henry Reginald Buller. *Researches on Fungi*, volume 2. Longmans, Green and Company, 1922.

[14] Anton Bary. *Comparative morphology and biology of the fungi, mycetozoa and bacteria*. Clarendon press, 1887.

[15] EJBZ Metchnikoff. Untersuchungen über die mesodermalen phagocyten einiger wirbeltiere. *Biol Zentralbl*, 3:560–5, 1883.

[16] Theodor Leber. Die entstehung der entzündung und die wirkung der entzündungerregenden schädlichkeiten: nach vorzugsweise am auge angestellten untersuchungen. 1891.

[17] Frank R Lillie. The production of sperm isoagglutinins by ova. *Science*, 36(929):527–530, 1912.

[18] Richard L Miller. Chemotaxis during fertilization in the hydroid campanularia. *Journal of Experimental Zoology*, 162(1):23–44, 1966.

[19] Marc Spehr, Gunter Gisselmann, Alexandra Poplawski, Jeffrey A Riffell, Christian H Wetzel, Richard K Zimmer, and Hanns Hatt. Identification of a testicular odorant receptor mediating human sperm chemotaxis. *Science*, 299(5615):2054–2058, 2003.

[20] Ross Granville Harrison. The outgrowth of the nerve fiber as a mode of protoplasmic movement. *Journal of Experimental Zoology*, 9(4):787–846, 1910.

[21] Timothy E Kennedy, Tito Serafini, JoséR De La Torre, and Marc Tessier-Lavigne. Netrins are diffusible chemotropic factors for commissural axons in the embryonic spinal cord. *Cell*, 78(3):425–435, 1994.

[22] Hans Spemann and Hilde Mangold. über induktion von embryonalanlagen durch implantation artfremder organisatoren. *Archiv für mikroskopische Anatomie und Entwicklungsmechanik*, 100:599–638, 1924.

[23] Kenshi Yoshida, Teruhisa Ozaki, Kenichiro Ushijima, and Hideo Hayashi. Studies on the mechanisms of invasion in cancer. i. isolation and purification of a factor chemotactic for cancer cells. *International Journal of Cancer*, 6(1):123–132, 1970.

[24] Maryse Bailly, Lin Yan, George M Whitesides, John S Condeelis, and Jeffrey E Segall. Regulation of protrusion shape and adhesion to the substratum during chemotactic responses of mammalian carcinoma cells. *Experimental cell research*, 241(2):285–299, 1998.

[25] H Hayashi, K Yoshida, T Ozaki, and K Ushijima. Chemotactic factor associated with invasion of cancer cells. *Nature*, 226(5241):174–175, 1970.

[26] Julius Adler. Chemoreceptors in bacteria: Studies of chemotaxis reveal systems that detect attractants independently of their metabolism. *Science*, 166(3913):1588–1597, 1969.

[27] Randall L. Johnson and Peter N. Devreotes. The cyclic amp receptor in dictyostelium discoideum. i. sequence of events following receptor activation. *The Journal of Cell Biology*, 88(3):734–740, 1981.

[28] H. C. Berg and E. M. Purcell. Physics of chemoreception. *Biophysical Journal*, 20(2):193–219, November 1977.

[29] William Bialek and Sima Setayeshgar. Physical limits to biochemical signaling. *Proceedings of the National Academy of Sciences of the United States of America*, 102(29):10040–10045, July 2005.

[30] Kazunari Kaizu, Wiet de Ronde, Joris Paijmans, Koichi Takahashi, Filipe Tostevin, and Pieter Rein ten Wolde. The Berg-Purcell limit revisited. *Biophysical Journal*, 106(4):976–985, February 2014.

[31] Robert G. Endres and Ned S. Wingreen. Accuracy of direct gradient sensing by cell-surface receptors. *Progress in Biophysics and Molecular Biology*, 100(1-3):33–39, October 2009.

[32] Bo Hu, Wen Chen, Wouter-Jan Rappel, and Herbert Levine. Physical limits on cellular sensing of spatial gradients. *Physical review letters*, 105(4):048104, 2010.

[33] Nicholas T. Henderson, Michael Pablo, Debraj Ghose, Manuella R. Clark-Cotton, Trevin R. Zyla, James Nolen, Timothy C. Elston, and Daniel J. Lew. Ratiometric GPCR signaling enables directional sensing in yeast. *PLoS biology*, 17(10):e3000484, October 2019.

[34] Alan Bush, Gustavo Vasen, Andreas Constantinou, Paula Dunayevich, Inés Lucía Patop, Matías Blaustein, and Alejandro Colman-Lerner. Yeast gpcr signaling reflects the fraction of occupied receptors, not the number. *Molecular systems biology*, 12(12):898, 2016.

[35] Vinal Lakhani and Timothy C. Elston. Testing the limits of gradient sensing. *PLoS computational biology*, 13(2):e1005386, February 2017.

[36] Masataka Yanagawa, Michio Hiroshima, Yuichi Togashi, Mitsuhiro Abe, Takahiro Yamashita, Yoshinori Shichida, Masayuki Murata, Masahiro Ueda, and Yasushi Sako. Single-molecule diffusion-based estimation of ligand effects on G protein–coupled receptors. *Science Signaling*, 11(548):eaao1917, September 2018.

[37] Harrie Hendriks. A Cramér-Rao type lower bound for estimators with values in a manifold. *Journal of Multivariate Analysis*, 38(2):245–261, August 1991.

[38] Debraj Ghose, Timothy Elston, and Daniel Lew. Orientation of Cell Polarity by Chemical Gradi-

ents. *Annual Review of Biophysics*, 51(1):null, 2022. _eprint: https://doi.org/10.1146/annurev-biophys-110821-071250.

[39] Khem Raj Ghusinga, Roger D Jones, Alan M Jones, and Timothy C Elston. Molecular switch architecture determines response properties of signaling pathways. *Proceedings of the National Academy of Sciences*, 118(11):e2013401118, 2021.

[40] Sally H Zigmond. Ability of polymorphonuclear leukocytes to orient in gradients of chemotactic factors. *Journal of Cell Biology*, 75(2):606–616, 1977.

[41] G Gerisch and U Wick. Intracellular oscillations and release of cyclic amp from dictyostelium cells. *Biochemical and biophysical research communications*, 65(1):364–370, 1975.

[42] Daniel R. Ballon, Paul L. Flanary, Douglas P. Gladue, James B. Konopka, Henrik G. Dohlman, and Jeremy Thorner. DEP-domain-mediated regulation of GPCR signaling responses. *Cell*, 126(6):1079–1093, September 2006.

[43] Christopher G Alvaro and Jeremy Thorner. Heterotrimeric g protein-coupled receptor signaling in yeast mating pheromone response. *Journal of Biological Chemistry*, 291(15):7788–7795, 2016.

[44] Anita Emmerstorfer-Augustin, Christoph M Augustin, Shadi Shams, and Jeremy Thorner. Tracking yeast pheromone receptor ste2 endocytosis using fluorogen-activating protein tagging. *Molecular biology of the cell*, 29(22):2720–2736, 2018.

[45] Christopher DC Allen, K Mark Ansel, Caroline Low, Robin Lesley, Hirokazu Tamamura, Nobutaka Fujii, and Jason G Cyster. Germinal center dark and light zone organization is mediated by cxcr4 and cxcr5. *Nature immunology*, 5(9):943–952, 2004.

[46] Abdelhak Belmadani, Phuong B Tran, Dongjun Ren, Stavroula Assimacopoulos, Elizabeth A Grove, and Richard J Miller. The chemokine stromal cell-derived factor-1 regulates the migration of sensory neuron progenitors. *Journal of Neuroscience*, 25(16):3995–4003, 2005.

[47] Michele K Dougherty, Jürgen Müller, Daniel A Ritt, Ming Zhou, Xiao Zhen Zhou, Terry D Copeland, Thomas P Conrads, Timothy D Veenstra, Kun Ping Lu, and Deborah K Morrison. Regulation of raf-1 by direct feedback phosphorylation. *Molecular cell*, 17(2):215–224, 2005.

[48] Piro Lito, Christine A Pratilas, Eric W Joseph, Madhavi Tadi, Ensar Halilovic, Matthew Zubrowski, Alan Huang, Wai Lin Wong, Margaret K Callahan, Taha Merghoub, et al. Relief of profound feedback inhibition of mitogenic signaling by raf inhibitors attenuates their activity in brafv600e melanomas. *Cancer cell*, 22(5):668–682, 2012.

[49] Ty M. Thomson, Kirsten R. Benjamin, Alan Bush, Tracy Love, David Pincus, Olga Resnekov, Roy C. Yu, Assaf Gordon, Alejandro Colman-Lerner, Drew Endy, and Roger Brent. Scaffold-mediated negative feedback regulates a yeast mapk pathway. *Molecular Systems Biology*, 7:460, 2011.

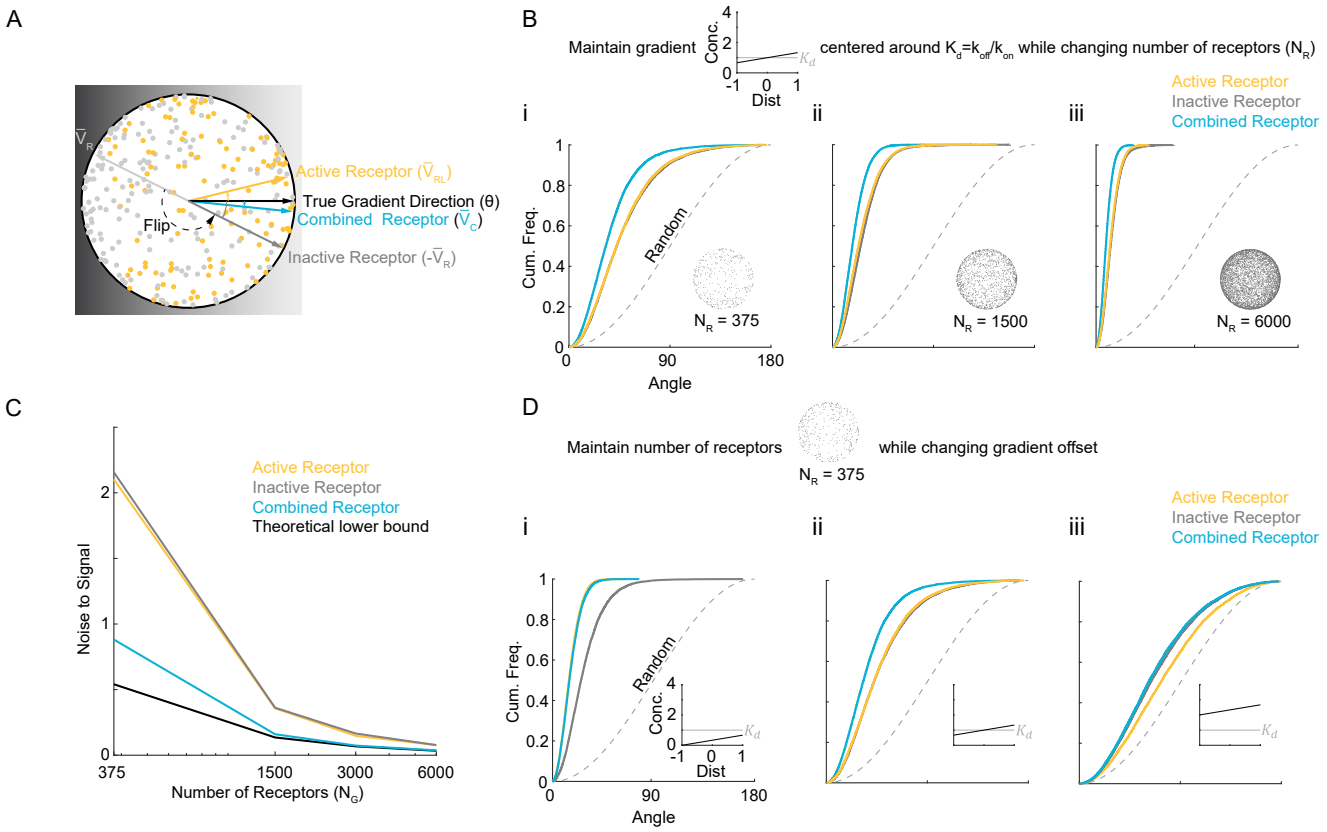

Figure 1: **Estimating gradient direction using information from both active and inactive receptors.** (**A**) Schematic depicting a spherical cell with receptors randomly distributed on its surface. Each receptor can be active (ligand-bound, yellow) or inactive (unbound, gray), and the gradient direction is inferred by summing receptor vectors and normalizing the sums to obtain unit vectors $\bar{V}_{RL}$, $\bar{V}_R$, and $\bar{V}_C$. Note that $\bar{V}_R$ is flipped to obtain $-\bar{V}_R$ to estimate gradient direction. (**B**) Cumulative distribution functions (CDFs) of angular error for the estimates $\bar{V}_{RL}$, $-\bar{V}_R$, $\bar{V}_C$, for three different receptor numbers ($N_R = 375$, 1500, 6000), where the gradient is centered around $K_d = 6nM$, ranging from $0.66\,K_d$ to $1.33\,K_d$. The dashed curve indicates the angular error for an estimate chosen uniformly at random over the cell. (**C**) Noise-to-signal ratio (NSR) comparing active-receptor sensing (yellow), inactive-receptor sensing (gray), and the combined-receptor estimate (blue) to the theoretical lower bound (black). Higher receptor counts reduce NSR, with the combined-receptor approach consistently outperforming either active- or inactive-only sensing. (**D**) Cumulative distribution functions (CDFs) of the angular error for the estimates $\bar{V}_{RL}$, $-\bar{V}_R$, $\bar{V}_C$ at fixed $N_R = 375$ but varying the gradient's offset relative to K_d: $C_0/K_d \in \{1/3, 1, 3\}$. As the mean concentration shifts, active and inactive receptors each capture different portions of the ligand profile, and combining their information again improves direction inference.

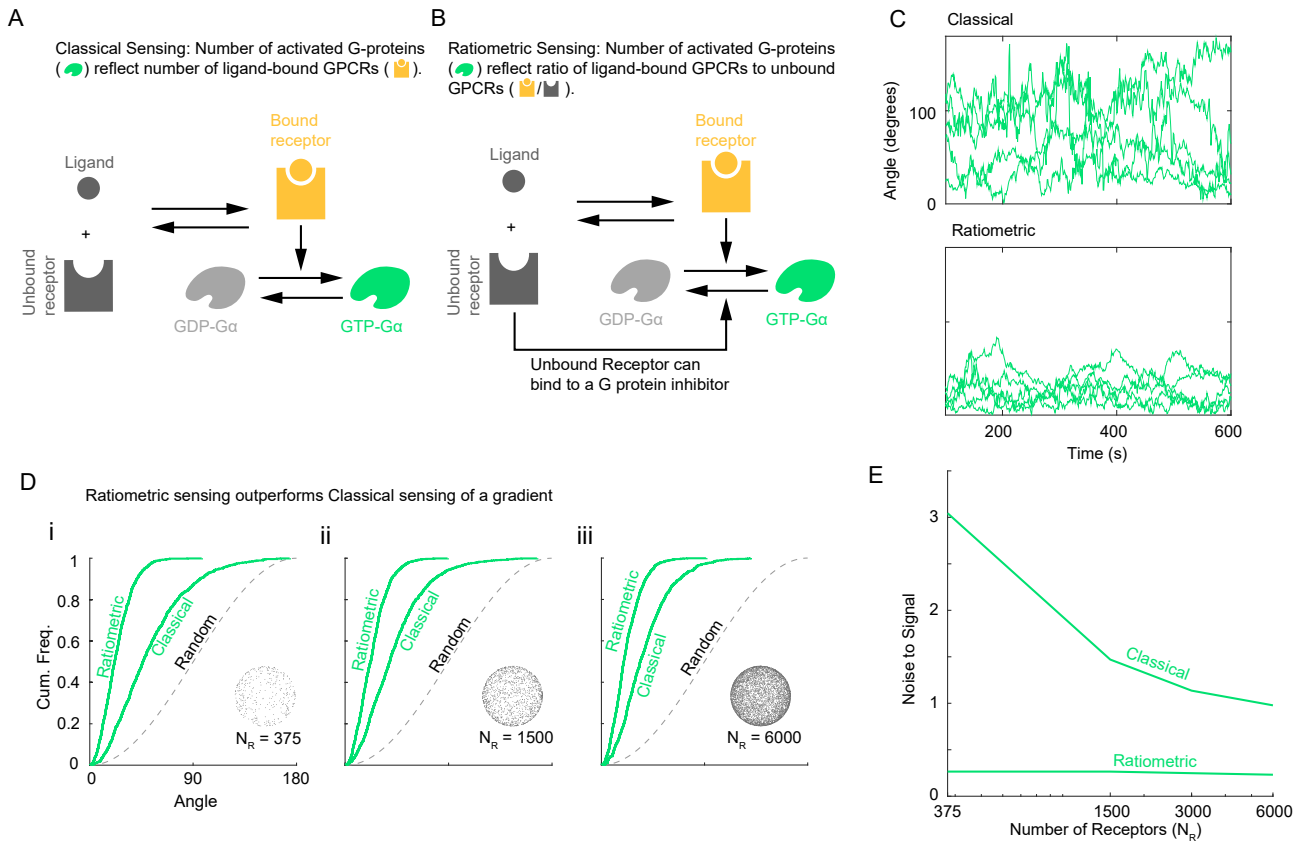

Figure 2: Ratiometric gradient sensing outperforms classical gradient sensing across a range of receptor numbers N_R. (**A**) Schematic of reactions that constitute classical sensing. (**B**) Schematic of reactions that constitute ratiometric sensing. (**C**) 5 sample traces each of direction derived from G protein distribution over time for ratiometric and classical sensing strategies. $N_R = 375$, $N_G = 2500$, $D_G = 0.002\mu m^2 s^{-1}$, $k_{on} = 0.0167 s^{-1} nM^{-1}$, $k_{off} = 0.1 s^{-1}$, $K_d = 6nM$. (**D**) Cumulative distribution functions of angular error comparing gradient sensing between ratiometric ($\bar{V}_G^r$) and classical ($\bar{V}_G^c$) scenarios. $N_R = [375, 3000, 6000]$ using the parameters in (C). (**E**) Noise to signal ratio of direction derived from G protein distribution compared between classical and ratiometric sensing strategies. $N_R = [375, 1500, 3000, 6000]$ using the parameters in (C). For classical sensing, the G protein off-rate was assigned according to $N_R \mapsto k_{go}$ as $[375, 1500, 3000, 6000] \mapsto [0.0083, 0.0357, 0.0769, 0.1687]\text{s}^{-1}$.

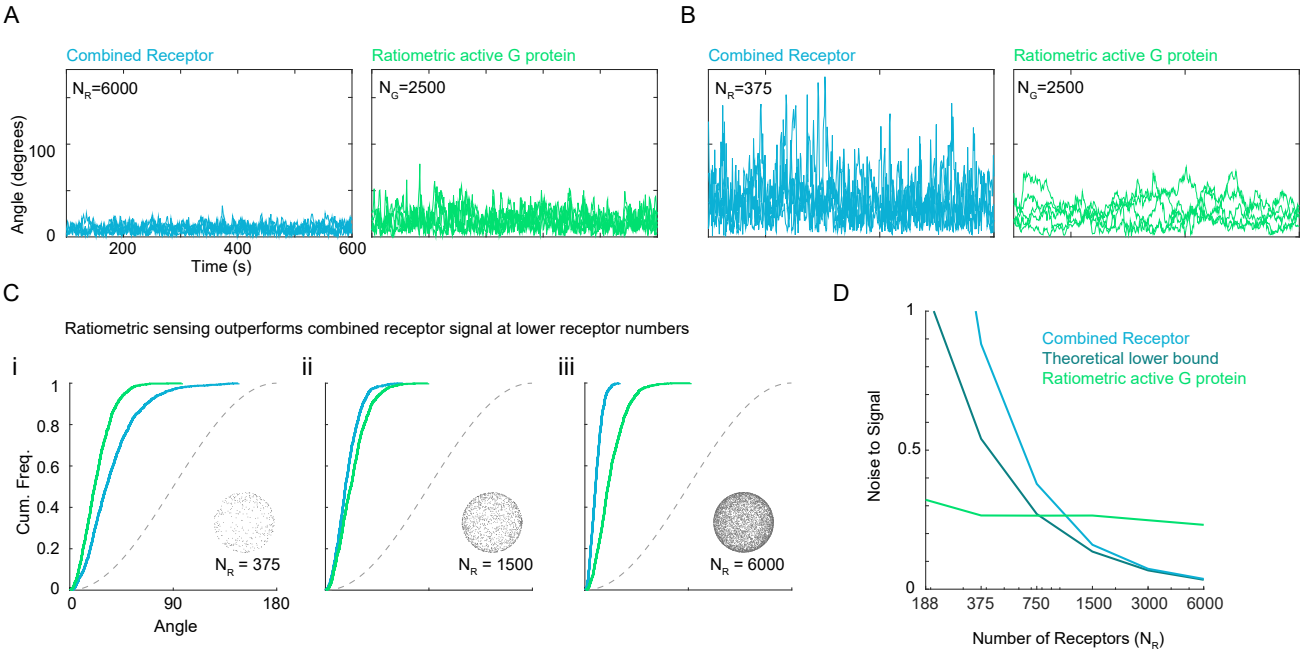

Figure 3: Ratiometric sensing allows G proteins to outperform theoretical limit. (**A**) Temporal tracks of V_C and V_G^r for $N_R = 6000$, $N_G = 2500$, $D_G = 0.002\mu m^2 s^{-1}$, $k_{on} = 0.0167 s^{-1} nM^{-1}$,$k_{off} = 0.1 s^{-1}$, $K_d = 6nM$. (**B**) Temporal tracks of V_C and V_G^r for $N_R = 375$ using parameters in (A). (**C**) Cumulative distribution functions of angular error comparing gradient sensing efficiency of active G protein in the ratiometric scenario to combined receptor. $N_R = [375, 3000, 6000]$ using parameters in (A). (**D**) Comparison of noise-to-signal ratio with theoretical Cramér-Rao bound which applies to the estimate V_C. For low values of N_R, the noise-to-signal ratio for V_G^r is below this theoretical bound, suggesting that V_G^r utilizes more information than is present in receptor states at a fixed time. $N_R = [188, 375, 750, 1500, 3000, 6000]$ using parameters in (A)

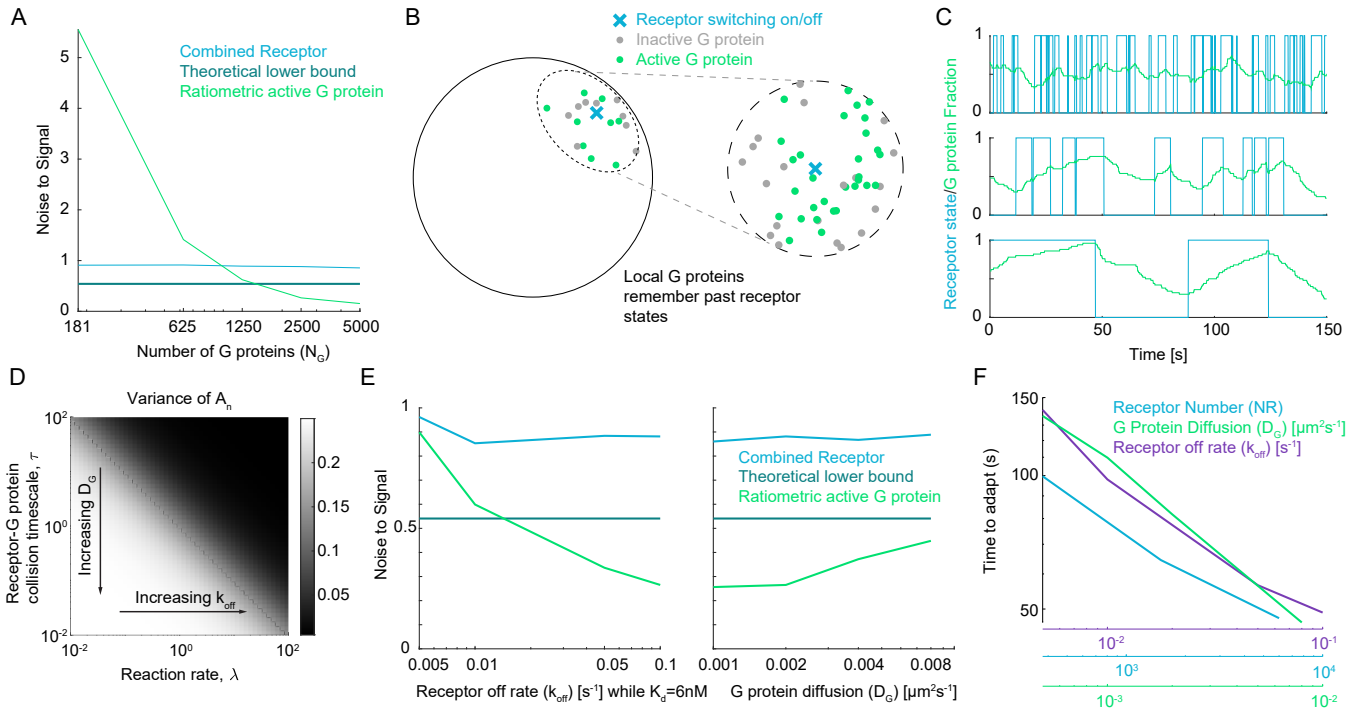

Figure 4: Ratiometric sensing enables G proteins to locally average past receptor states. (**A**) Noise-to-signal ratio for V_G^r, V_C, and the theoretical lower bound as a function of the number of G proteins. $N_G = [181, 625, 1250, 2500, 5000]$, $N_R = 375$, $D_G = 0.002\mu m^2 s^{-1}$, $k_{on} = 0.0167 s^{-1} nM^{-1}$,$k_{off} = 0.1 s^{-1}$, $K_d = 6nM$. (**B**) Cartoon of a single receptor surrounded by G proteins that have recently inherited the receptor's state. (**C**) Time series showing a receptor switching state (blue) at different rates, along with fraction A_n of G proteins that are active (green). With faster receptor dynamics, A_n exhibits less fluctuation. (**D**) Phase plot showing the variance in the fraction of active G proteins for different values of the timescales for receptor switching or diffusion. (**E**) Gradient sensing accuracy increases with faster receptor switching rates and decreases with higher diffusion constants. $N_G = 2500$, $N_R = 375$. Left: $k_{off} = [0.005, 0.01, 0.05, 0.1]\ s^{-1}$. Right: $D_G = [0.001, 0.002, 0.004, 0.008]\ \mu m^2 s^{-1}$. (**F**) Time it takes for a cell to adapt to a gradient being flipped 180 degrees. Default values: $N_G = 2500$, $N_R = 375$, $k_{off} = 0.1 s^{-1}$, $k_D = 6nM$, and $D_G = 0.002\mu m^2 s^{-1}$. Ranges for changing parameter: $N_R = [375, 1500, 6000]$, $k_{off} = [0.005, 0.01, 0.1]\ s^{-1}$, and $D_G = [0.001, 0.002, 0.004, 0.008]\ \mu m^2 s^{-1}$.